

B. TECH. PROJECT REPORT

On

FE Modeling of Wire and Arc Additive Layer Manufacturing Process

BY

Abhishek Kumar

Soorya Pratap

Apoorv Agarwal



**DISCIPLINE OF MECHANICAL ENGINEERING
INDIAN INSTITUTE OF TECHNOLOGY INDORE**

December 2019

FE Modeling of Wire and Arc Additive Layer Manufacturing Process

A PROJECT REPORT

*Submitted in partial fulfillment of the
requirements for the award of the degrees*

of
BACHELOR OF TECHNOLOGY
in
MECHANICAL ENGINEERING

Submitted by:

Abhishek Kumar (160003002)

Apoorv Agrawal (160003009)

Soorya Pratap (160003054)

Guided by:

Dr. Indrasen Singh (Assistant Professor, IIT INDORE)



INDIAN INSTITUTE OF TECHNOLOGY INDORE

December 2019

CANDIDATE'S DECLARATION

We hereby declare that the project entitled **FE Modeling of Wire and Arc Additive Layer Manufacturing Process** submitted in partial fulfillment for the award of the degree of Bachelor of Technology in Mechanical Engineering completed under the supervision of **Dr. Indrasen Singh**, Assistant Professor in Mechanical Engineering Department, IIT Indore is an authentic work.

Further, we declare that we have not submitted this work for the award of any other degree elsewhere.

Abhishek Kumar (160003002)

Apoorv Agrawal (160003009)

Soorya Pratap (160003054)

CERTIFICATE by BTP Guide(s)

It is certified that the above statement made by the students is correct to the best of my knowledge.

Dr. Indrasen Singh

Preface

This report on “FE Modeling of Wire and Arc Additive Layer Manufacturing Process” is prepared under the guidance of Dr. Indrasen Singh.

Additive Manufacturing is a novel technique which fabricates 3D components in a layer by layer fashion. It was originally developed for Rapid prototyping and Rapid Tooling which are the processes of producing functional prototypes and null-series for tests with metal or higher grade plastics. In the recent years, AM techniques have been moved to Rapid Manufacturing to meet the requirement of producing end-use parts with near-net shape and full functionality. Great research interests were induced on this novel process because of its significant benefits of time saving, material saving, flexibility, and more friendly to environment. There are various techniques employed for metal additive manufacturing depending on energy source and type of raw materials used. Amongst all, Wire+Arc Additive Manufacturing seems to be the best candidate for the manufacturing of medium to large scale components, thanks to the relatively high deposition rates, potentially unlimited build volume, low BTF ratios and low capital and feedstock costs. However, it has been seen that the high heat input and the non uniform expansion and contraction of material during thermal cycle results in thermal stresses and significant distortion. Therefore, the analysis of the manufacturing process should be done to get some predictions about the distortions and the stresses developed in the components. Parameter study, kinematic setup for such working volumes and thermal analysis of deposition process to minimize distortions are some of the related aspects. Studies on different deposition parameters, deposition sequences and deposition strategies are also carried out. We have tried to the best of our abilities and knowledge to explain the content in a lucid manner. We have also added 3-D models and figures to make it more illustrative.

Abhishek Kumar (160003002)

Soorya Pratap (160003054)

Apoorv Agrawal (160003009)

B.Tech. IV Year

Discipline of Mechanical Engineering

IIT Indore

Acknowledgements

We will first wish to thank Dr. Indrasen Singh for his kind support and valuable guidance. The door to Dr. Indrasen Singh's office was always open whenever we had any issue or any kind of doubts related to our project work. He motivated us in the right direction at tough times. We will also thank the people whose papers for literature survey we used to have better depth about our project. Also, We would like to thank Mr. Hirmukhe Sidram (Ph.D. scholar), Harshdeep Singh (M.tech student) and Mr. Kailash Patel, CAD lab incharge, for their valuable time and support.. Finally, We feel grateful to express our thankfulness to our parents and friends to empower us with continuous support while writing this thesis. This accomplishment seems hard to imagine without their help and support.

It is their help and support, due to which we became able to complete the design and technical report.

Without their support this report would not have been possible.

Abhishek Kumar (160003002)

Soorya Pratap (160003054)

Apoorv Agrawal (160003009)

B.Tech. IV Year

Discipline of Mechanical Engineering

IIT Indore

Abstract

Conventional manufacturing processes which often result in a high rate of machining cannot satisfy the continuously increasing requirements of a sustainable, low cost, and environmentally friendly modern industry. Thus, Additive Manufacturing (AM) has become an important industrial process for the manufacture of custom-made metal workpieces. The AM process takes CAD data and converts it into layers and then CNC language and process parameters. Among the different AM Processes, Wire Arc Additive Manufacturing (WAAM), is a very promising technology that enables complex shaped big part manufacturing of high added value materials. This technology is part of the additive layer manufacturing processes which uses metallic wires as raw material and an electric arc as energy source. WAAM process has important advantages over other conventional machining processes, such as high resource efficiency, high productivity and low equipment cost. In this process, 3D metallic components are built by depositing beads of weld metal in a layer by layer fashion. WAALM can be used to deposit a variety of materials that can be welded, such as steel, Ni alloys, and Ti alloys. However, the high heat input and the non-uniform expansion and contraction of the material during the thermal cycle results in residual stresses and significant distortion. So, important factor that need to be considered when one decides the deposition parameters and build path are the residual stresses and distortions generated during the WAAM process. Although these thermally induced issues are unavoidable for the WAAM process, using a proper deposition parameter and build path can control the residual stresses and minimise the distortion level without any extra process. Therefore, a numerical model needs to be developed which can provide predictions of the residual stresses and the distortions of the WAAM components. This thesis aims on the thermo-mechanical analysis of the WAAM process using the FE approaches, with a special research focus on the efficient FE modelling approaches for large WAAM components. Therefore, to be capable of analysing the thermo-mechanical behaviour of large-scale WAAM components, an efficient FE approach was developed which can significantly reduce the computational time. Finally, the accuracy of the model was validated against the transient model as well as experimental measurements. So ,with the help of the FE models, studies on different deposition parameters, deposition sequences and deposition strategies were carried out. It has been proved that the residual stresses and the distortions are possible to be reduced by using optimised deposition parameters and sequences got with the help of the thermomechanical analysis of the WAAM process.

Table of Contents

Candidate's Declaration.....	3
Supervisor's Certificate.....	3
Preface.....	5
Acknowledgements.....	6
Abstract.....	7
List of figures and Tables.....	9
Chapter 1: Introduction.....	10
Chapter 2: Literature Review	14
Chapter 3: Thermomechanical FE Analysis of WAALM.....	21
Chapter 4: Results and Conclusions.....	32
References.....	42

List of Figures

Figure 1-1 : Components built by the WAAM process: (a) shell castings; (b) part with crossovers and intersections; (c) Ti aerospace component.

Figure 2-1: AM fabricated fuel nozzle for Jet engine, Complex geometry design, Aerospace part, Blades design

Figure 2-2: Classification of Metal AM

Figure 2-3: Steps for AM process: (a) CAD model (b) Numerical slicing (c) Layer processing for a single layer (d) Layer processing for all layers and (e) Finished component

Figure 2-4: Temperature and stress field around the welding source

Figure 2-5: Temperature stress histories for different material points: (a) point X is at the edge of the weld pool; (b) point Y is slightly further from the weld pool.

Figure 2-6: Longitudinal stress across weld centreline

Figure 3-1 : Model along with its dimensions shown

Figure 3-2: Biased meshes shown in the model

Figure 3-3 : Goldak's double ellipsoidal heat source model

Figure 3-4: Depositions of the beads one by one using element birth technique

Figure 3-5 :The parameter settings for the Goldak double ellipsoidal heat source model. (a) Metallographic profile shows the settings for b and c; (b) weld pool surface ripple markings for a_r and a_t

Figure 3-6 : Thermal Boundary conditions

Figure 3-7: Procedure of transient thermo-mechanical modelling of the WAAM process.

Figure 4-1: Nodes positions to know their Temperature histories

Figure 4-2: Temperature Histories using FEM & verification on the measuring positions (a) at TP1,(b) at TP2 & (c) at TP3

Figure 4-3: Longitudinal stress predictions of the 4 layer WAAM wall component: (a) with clamps; (b) cross section of (a); (c) after clamps are removed (deformation factor: 5); (d) cross section of (c).

Figure 4-4: Verification of Distortion along Longitudinal Direction

Figure 4-5: (a) Principal stress distribution along Transverse direction with 1 layer deposition, (b) Principal stress distribution along Transverse direction with 2 layers deposition, (c) Principal stress distribution along Transverse direction with 3 layers deposition.

Figure 4-6: Variation of Longitudinal Stresses along Z-direction (4 Layers of 2 mm each)

List of Tables

Table 3-1 : Detailed thermal properties of S355

Table 3-2 : Detailed temperature-dependent thermal expansion coefficient, and Poisson's ratio of S355

Table 3-3 : Detailed temperature-dependent Young's Modulus, and yield strength for the filler material and base plate

Chapter 1

INTRODUCTION

1.1 Research Background



Conventional manufacturing processes which often result in a high rate of machining cannot satisfy the continuously increasing requirements of a sustainable, low cost, and environmentally friendly modern industry. Thus, Additive Manufacturing (AM) has become an important industrial process for the manufacture of custom-made metal workpieces. The AM process takes CAD data and converts it into layers and then CNC language and process parameters. In this way, freeform components can be fabricated. As shown in Figure 1-1 the basic metal AM system comprises four parts: CNC controller, motion system, heat source for melting the metal and a material supply system. Current commercial metal AM systems are based around power beam heating sources (usually lasers) and material supply in the form of powder, most commonly in the form of a powder bed. In this approach a roller is used to add a layer of metallic powder and the laser is scanned over the surface of the powder fusing or melting a patterned layer. The same process is repeated for the subsequent layers until the component reaches the designed height. This kind of systems are capable of producing extremely complex structures and enable either weight saving or added functionality to existing or future components. These systems feature build rates of a few tens of grams per hour and build volumes typically $0.3 \times 0.3 \times 0.3 \text{ m}^3$. Due to the sensitivity of powders to contamination and for safety reasons, all power beam systems need an environmental chamber (known as in-chamber) filled with an inert gas. Consequently AM components

made by these methods have a very high build cost because of the system complexity and the slow build rates. As a result the market for these systems is limited to niche areas such as medical implants, small complex high value parts (e.g. engine components) and jewellery.

A promising breakthrough for metal AM technology is the Wire and Arc Additive Manufacture (WAAM) process which combines electric arc heating sources with a metallic wire feeding system. In the WAAM process, 3D metallic components are built by depositing beads of weld metal in a layer by layer fashion. The WAAM system can be built by combining the standard wire based welding equipment and the common motion system such as industrial robots and gantries. The WAAM system can also be easily retrofitted onto existing machine tools which is capable of both deposition and machining. The hardware cost for the WAAM system is typically an order of magnitude less than the laser powder systems and it can achieve deposition rates two orders of magnitude higher than laser powder systems (typically 2-4 kg/hour). In the current research of the WAAM process, a local shielding technique is utilised for fabricating the highly reactive metallic components. As an environmental chamber is not necessarily required (out-of-chamber), the build volume is unlimited. Various materials that are weldable can be used in the WAAM process, such as steel, Ni alloys, Al alloys and Ti alloys. The WAAM system allows the production of large custom-made and low volume metal workpieces with high deposition rates. Specific components have been produced as required by industrial partners using the WAAM process. Figure 1-1 (a) shows the building of four mild steel projectile casings each with a mass of 32 kg. The deposition rate for building these parts is 3.31 kg/h. Figure 1-1 (b) shows a part illustrating that components with numerous crossovers and intersections can be built using WAAM process. Figure 1-1 (c) shows a typical titanium aerospace part that has been built using the WAAM process. This component highlights the benefits of the WAAM process over the current process of machining from billets for these kinds of parts. The final component weight is 6.2 kg and to machine from a solid would require a starting billet weight of 27 kg which gives a buy-to-fly ratio of over 4. This is extremely wasteful in terms of material. In contrast using the WAAM process the base plate has a weight of 5 kg and 1.5 kg of material is added with 0.3 kg machined away to get the final profile. This gives a material saving of 19.3 kg and a buy-to-fly ratio of near to 1. The deposition time for this part is only 1 hour.



Figure 1-1 : Components built by the WAAM process: (a) shell castings; (b) part with crossovers and intersections; (c) Ti aerospace component.

One important factor that need to be considered when one decides the deposition parameters and build path are the residual stresses and distortions generated during the WAAM process. Although these thermally induced issues are unavoidable for the WAAM process, using a proper deposition parameter and build path can control the residual stresses and minimise the distortion level without any extra process. Therefore, a numerical model needs to be developed which can provide predictions of the residual stresses and the distortions of the WAAM components. This thesis aims on the thermo-mechanical analysis of the WAAM process using the FE approaches, with a special research focus on the efficient FE modelling approaches for large WAAM components.

1.2 Problem Statement

We know that Metal additive manufacturing have been in trend due to its ability to produce components at reduced cost and low buy-to-fly ratio. However, the non-uniform expansion and contraction of the materials during the thermal cycles result in residual stresses. It is accompanied with distortions which are one of the most problematic issues arising from the WAAM process. Therefore, it is highly important to understand the thermomechanical performance during the WAAM process, and moreover, to improve the WAAM process to reduce the residual stress and distortion level.

Finite Element (FE) analysis is a common method to study the thermomechanical performance of the AM process. The most widely used FE analyses of AM processes utilise transient models with a moving heat source. Element birth technique is used for simulating addition of material, providing accurate predictions. However, the transient aspect and the highly non-linear material behaviour result in long computational time, and hence the models

are usually limited to a small scale. To investigate large-scale WAAM components, which can scale to several meters, this conventional transient FE approach is not suitable. Efficient FE approach needs to be developed to provide fast estimations of the temperature distribution, residual stresses and distortions. The efficient FE model will be helpful for deciding the best deposition parameters and build strategies.

1.3 Outline

The thesis comprised of the following chapters-

Chapter 1 : This chapter comprises of the Introduction and the background research stating the problem statement.

Chapter 2 : The chapter summarises the literature about the themes which are required for the project.

Chapter 3 : This chapter will explain the Transient FE Analysis of the WAALM process

Chapter 4 : This chapter will explain the Results and conclusions obtained from the FE analysis.

Chapter 5 : This chapter will give some ideas for the future scope of the project we did.

Chapter 2

LITERATURE REVIEW

2.1 ADDITIVE MANUFACTURING



Metal additive manufacturing has been in trend due to its ability to produce components at reduced cost and low buy-to-fly ratio. There are various techniques employed for metal additive manufacturing depending on energy source and type of raw materials used. Based on raw materials, metal additive manufacturing can be classified as wire-based, powder-based and sheet-based (laminated object manufacturing). Amongst these three, wire based systems have higher material efficiency and high deposition rates. They are also better suited for continuous and uncluttered material supply. Hence, they are most suitable for large components. These wire based systems can be used in conjunction with different energy sources like Laser, Electron Beam and Arc. WLAM (wire and laser based additive

manufacturing), EBAM (electron beam additive manufacturing) and WAAM (wire and arc based additive manufacturing) are examples of each of these energy sources respectively. This section is about WAAM and its comparison with other powder and wire based systems and the application of metal additive manufacturing. Wire and arc additive manufacturing is a center of attraction now a days due to higher deposition rates, with added freedom of selection of power source as well its manipulation. The facility with the wire and arc manufacturing provided to get the desired properties at different locations is due to ability to change deposition parameters like current voltage and wire feed rates etc. Wire and arc additive manufacturing specially GMAW based has the potential to build large objects due to its ability to provide higher deposition rates. Arc based welding depositions is preferred over electron beam and laser based AM because it is more economical as well as faster.

In WAAM wire and arc manufacturing components are made by deposition by bead of metal welds layer by layer using GMAW welding explained above and utilizing a position system like a CNC positioning system. Main advantage of wire and arc manufacturing additive manufacturing is high deposition rate so it is able to reduce manufacturing as well as lead time. Despite of higher deposition rates better economics and speed of the process GMAW based AM has some major areas of concern when implementing for bigger products issues being residual stresses due to temperature gradient because of successive layer deposition layer stability due to slower solidification for larger layers, surface roughness which can go on accumulating due to scallops, substrate or base plate distortion as well as risk of welding defects.

2.2 Applications of Metal Additive Manufacturing

Initially considered as sheer tool of prototyping and modelling AM has now expanded its domain of applications in so much wider domains. From initial prototyping or tooling to the final product modern industries like architectural, medical, dental, aerospace, automotive, furniture and jewellery, new and innovative applications are constantly being developed. The major application of AM lies in following domains.

- Model and Prototype fabrication.
- Medical equipments, automobiles and aerospace sector.
- For job order short term production where tooling cost for conventional processes is higher

- Fabrication of complex geometries.

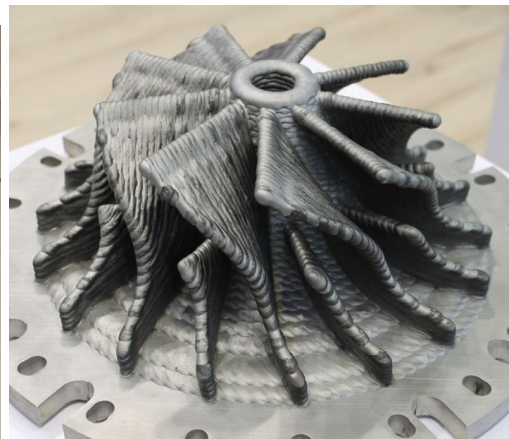
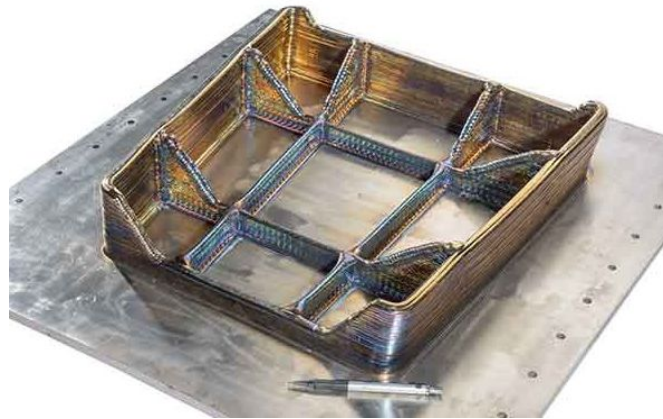


Figure 2-1: AM fabricated fuel nozzle for Jet engine, Complex geometry design, Aerospace part, Blades design

Some other big area applications of metal AM involves in jet engines, rockets, oil and gas equipments, turbine blades, nuclear components, marine application etc. Also aircraft structures frames and parts can be manufactured using EBAM and WAAM techniques.

2.3 Classifications of Metal AM Methods

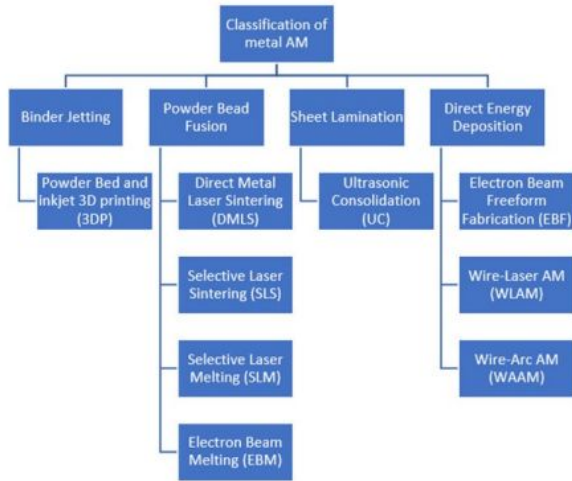


Figure 2-2: Classification of Metal AM

Classified by the type of the heat sources AM techniques contains several groups, such as Laser Melting (LM), Ultrasonic Additive Manufacturing (UAM), Electron Beam Melting (EBM), Plasma Deposition (PD), and Gas Metal Arc Welding (GWAM) etc. Metallic wire and metallic powder are the two main material feeding methods. By combining the different heat sources with different material feeding methods various AM techniques have been developed.

The combination of laser and powder is probably the most widely applied option. With the highly focused laser power and accurately controlled powder feeding, the parts can be fabricated with detailed features and with high accuracy. However, the low deposition rate and the complexity of the system constrain the dimension of the AM parts to a rather small scale. Moreover, a lot of quality issues can be raised in the powder system, such as non-fully dense parts, the mechanical properties are not consistent in all directions, and pore formation. In addition, only part of the powder can be actually used which cause an issue of waste material.

Wire based AM process is gaining more favour because of its higher deposition rates and higher efficiency. The deposition of metallic wire with high power diode laser was studied by Syed and Li on mild steel and by Mok et al. on Ti-6Al-4V. High power fibre laser has been considered as the heat source for the deposition of Ti-6Al-4V wire because of its high efficiency, low maintenance cost, and the flexibility in beam position and manipulation. Fully dense components can be fabricated using this process.

2.4 Procedure for the WAAM

Additive manufacturing application is limitless. Earlier Additive manufacturing was used in the form of Rapid Prototyping for producing prototype of actual working model. Now a days,AM is being used to fabricate functional user products in aircraft, dental restorations, medical implants, automobiles, and even fashion products. Additive manufacturing makes it possible to manufacture a 3D object out of 3D cad model by realizing one layer at a time. STL format is sliced and tool path generation strategies are made then each layer is realized at a time and thus layer by layer complete formation of the object is done. The basic steps for additive manufacturing is shown below.

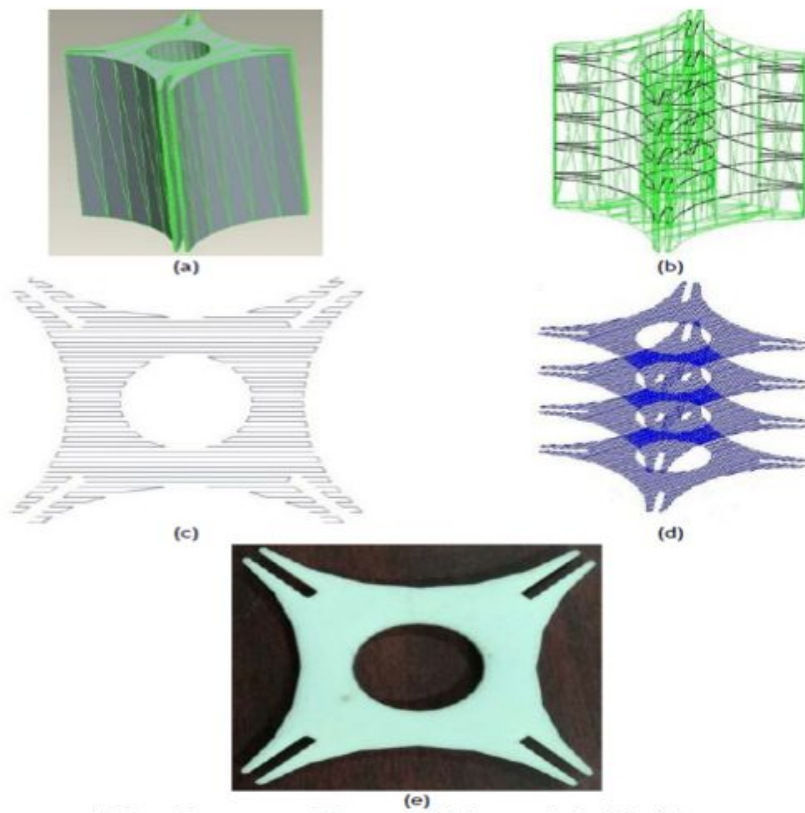


Figure 2-3: Steps for AM process: (a) CAD model (b) Numerical slicing (c) Layer processing for a single layer (d) Layer processing for all layers and (e) Finished component

2.5 Thermomechanical issues during deposition process

A large area of compressive stress is generated in front of the fusion zone due to the thermal expansion of the heated material which is being constrained by the surrounding cold material. The stress in the fusion zone is very low because of the significantly reduced yield stress level by the high temperatures. After the heat source passes, the heated material cools down in a short time. It results in tensile stresses in the region behind the heat source due to the contraction of the cooling material, and this material contraction is restrained by the surrounding cold material which consequently results in tensile stresses. If the tensile and compressive stresses exceed the yield limit then plastic stress generates.

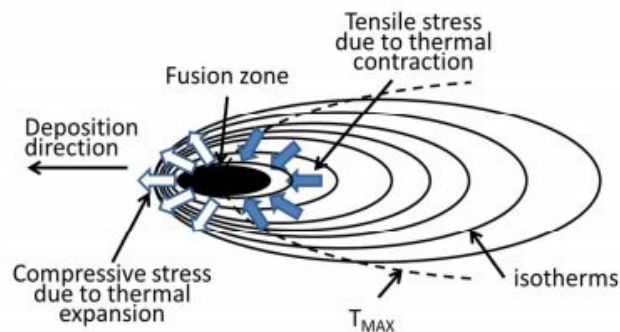


Figure 2-4: Temperature and stress field around the welding source

To explain how residual stresses generate, the longitudinal stress and temperature histories for two points are schematically illustrated in Figure 2-5. Point X is located at the edge of the weld pool while Point Y is slightly further away from the weld pool but is still in the region where the residual stress generates. As the heat source approaches, the temperature of both points rises. As a consequence of the metal expansion a compressive stress generates, first appears elastically as shown by line AB in both figures of Figure 2-5, and then turns into plastic flow when it exceeds the yield limit as shown by line BC. After the heat source passes, the temperature of the material drops and a tensile stress develops due to the contracting material being restrained by the surrounding material. In the case of Point Y all the tensile stress is accommodated elastically with no plastic flow occurring as shown by the line CD in Figure 2-5 (b). In the case of Point X some of the tensile stress exceeds the yield limit and develops plastic flow as shown by the line DE in Figure 2-5 (a). When the material has cooled back down to room temperature a tensile residual stress is present as shown by the large grey arrows in both figures of Figure 2-5.

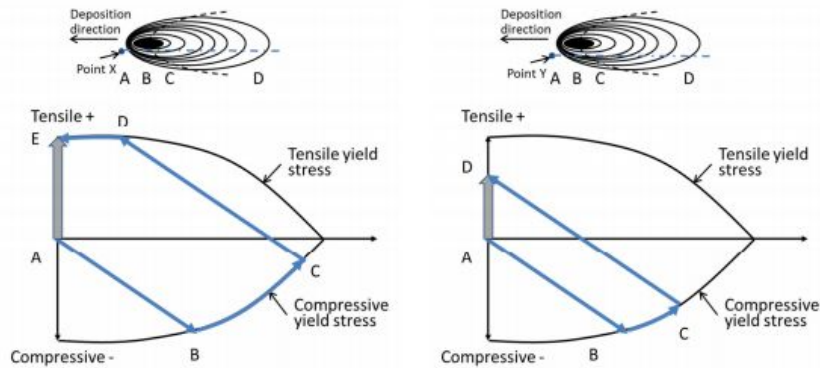


Figure 2-5: Temperature stress histories for different material points: (a) point X is at the edge of the weld pool; (b) point Y is slightly further from the weld pool.

A typical longitudinal residual profile for the mild steel across the weld centreline is shown in Figure 2-6. The high tensile stresses (reaching the yield limit) distribute in the region adjacent to the weld centreline (as explained by Figure 2-5 (a)).

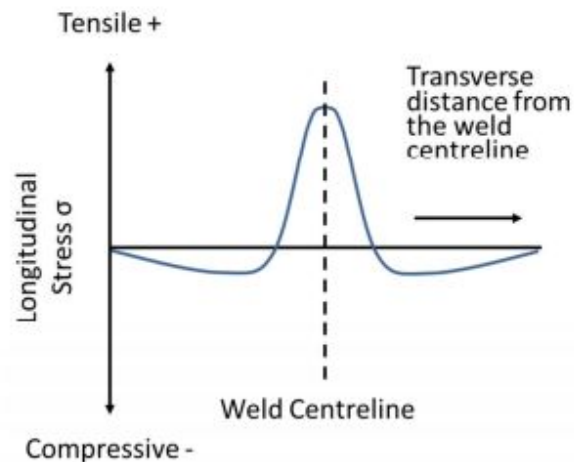


Figure 2-6: Longitudinal stress across weld centreline

Classified by different directions, residual stresses contain three components. These are the longitudinal stress in the direction of welding, transverse stress which is perpendicular to the direction of welding and normal stress through the thickness of the material. The longitudinal stress is usually the dominant component among the residual stresses due to the significant longitudinal contraction of the weld as it cools down. The normal stress is usually comparatively small due to the small variation in temperature and small material restrains in the thickness direction.

Chapter 3

THERMOMECHANICAL FE ANALYSIS OF WAALM

Thermal study and analysis is one of the most crucial aspects for design of thermally driven wire and arc additive manufacturing. This section takes into account the thermal behaviour of the plate- WAAM manufactured component with multi-pass welds and successively deposited layers.

3.1 Modelling Procedure

A thermo-mechanical analysis has to be carried out in 2 steps. The first step involves transient state thermal history analysis (time-temperature analysis) from which the nodal temperature history is carried and utilized for the mechanical analysis. This is helpful in prediction of thermal stress and distortion. Below is the model which was input for the analysis in the ABAQUS software.

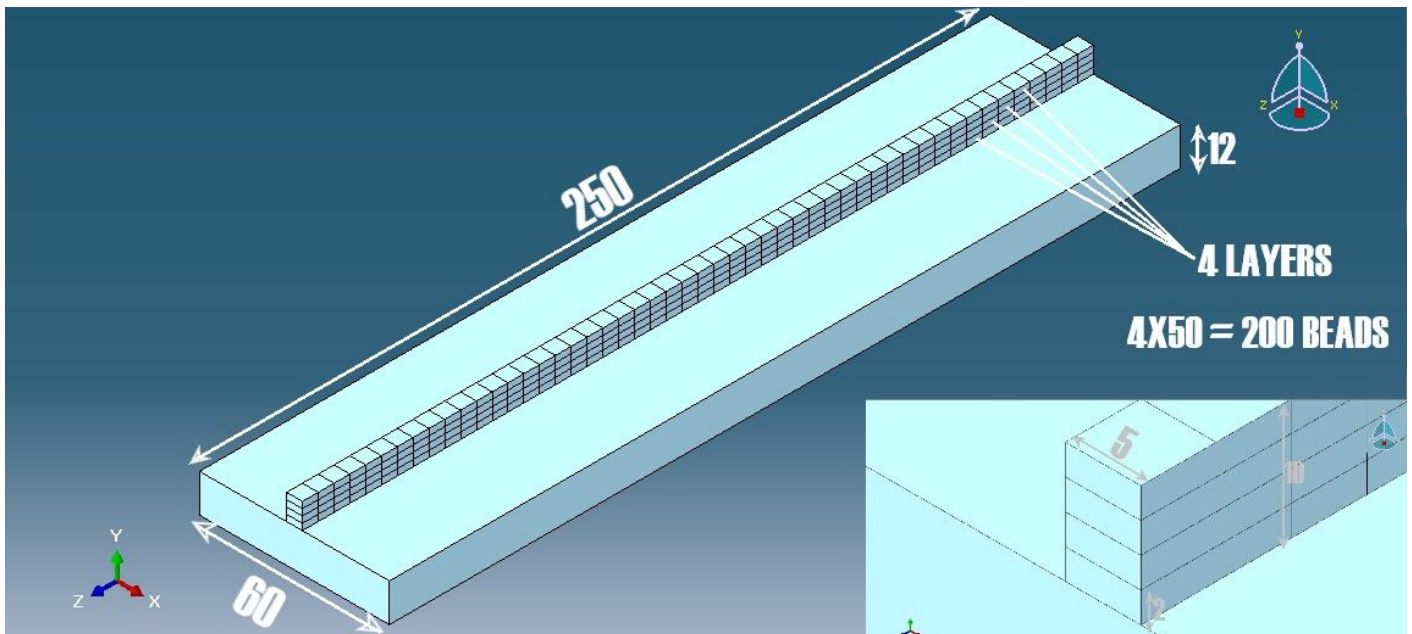


Figure 3-1 : Model along with its dimensions shown

The width and thickness of the base plate used in this study were the same to those used in the experiment, which were 60 mm and 12 mm respectively. The length of the base plate was set to 500 mm. One layer of deposited material is modelled on top of the base plate which was 2 mm in height and 5 mm in width.

Models of the very accurate simulation category should be chosen if details around the weld pool are of interest. Finer meshes, smaller time steps and more detailed material models and heat input models are required for the models with higher accuracy. It is recommended to use temperature dependent thermal and mechanical material properties for all accuracy categories. Three aspects of the material model, including cut-off temperature, the effect of phase and microstructure changes, and the rate dependent plastic behaviour at higher temperatures, need to be considered differently for achieving different accuracy levels. The use of cut-off temperature is firstly due to the scarce experimental data for the high temperatures and secondly because of the convergence difficulty of the FE model caused by the soft material performance in the high temperature. The cut-off temperature is set as the upper limit of the temperature in the mechanical analysis, and no changes in the mechanical material properties are accounted above the cut-off temperature. Volume changes due to phase changes can be ignored in the basic simulation, while the effects of phase changes on material properties are recommended to be included in the models for higher accuracy levels.

3.1.1 Finite element Meshing

The number and size of the FEM meshes can significantly influence the accuracy of the model and the computational time. With the same circumstances using smaller meshes in the model intend to give more accurate results. However, long calculating times and huge data storage space are required for completing the job. Thus, a balanced meshing strategy should be used to get the temperature and stress fields with acceptable accuracy while having the fewest number of elements in the model.

Because the materials of the weld bead and in the Heat Affected Zone (HAZ) experience high temperature gradients, dense meshes were utilised in this area. **Biased meshes** were used for the base plate in the y and z directions as shown in Figure 3-2. The density of the elements decreases gradually as it goes far apart from the HAZ region. Nearly all the researchers use biased meshes in the welding simulation. To apply the heat flux more accurately, dense meshes are adopted in the weld zone and its vicinity. The element size

increases progressively with distance from the weld centreline on the direction perpendicular to the direction of welding and through thickness.

Below is the model showing the biased meshing in the model-

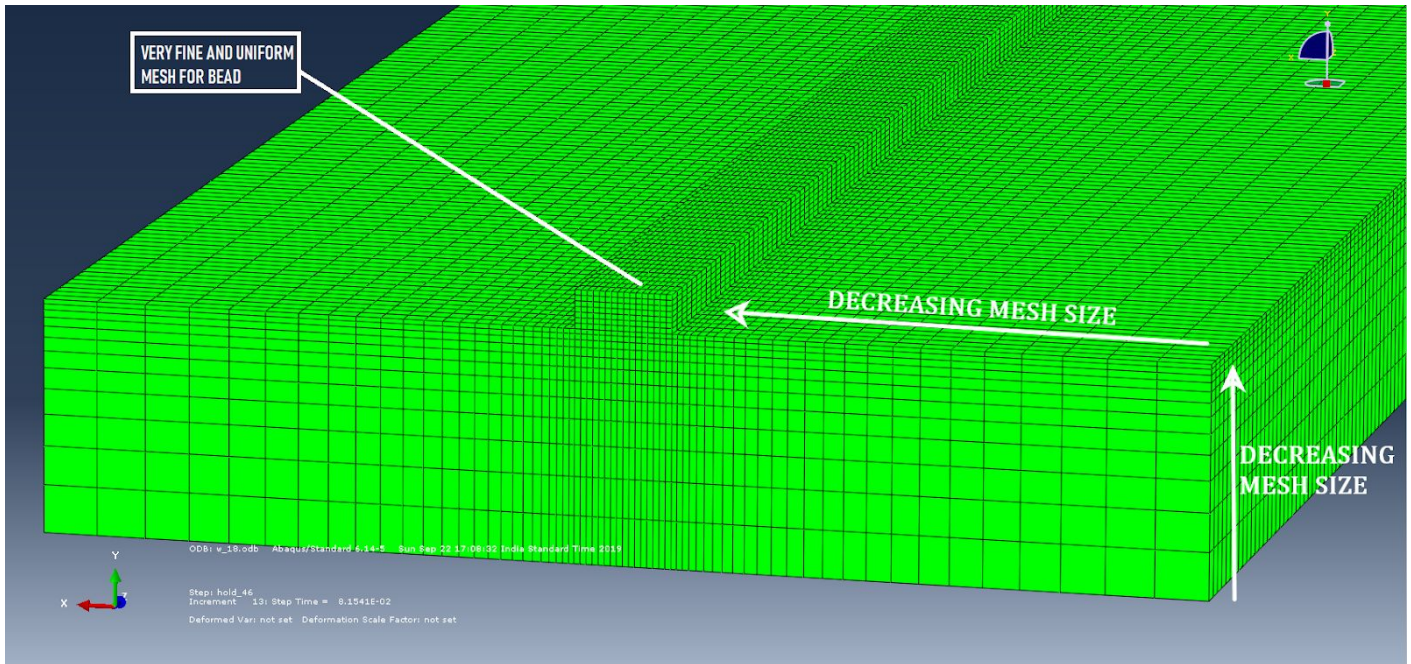


Figure 3-2: Biased meshes shown in the model

3.1.2 Heat Source Model

Heat source modelling is most crucial aspect for any welding based modelling process. For an incompressible body heat flow is characterised by flow from higher temperature to lower temperature. The heat flow thus occurring in transient in nature and this transient temperature variation $T(x,y,z,t)$ drives the physical attributes of the welded component and characterize melting and solidification melting and remelting and HAZ . Mechanisms through which micro-structures of the weld change, and therefore control the changes, it is crucial to understanding the heat distribution from the torch, and the dissipation of this heat through welding geometry. For welding processes in which the momentum transfer effect of the arc on the weld pool is large, Goldak et al. (1984) derived a model to describe the volumetric heat flux acting on a substrate due to arc. In order to overcome the discrepancy between the predicted and measured temperature gradients in front and behind the arc, two ellipsoidal heat sources were combined as shown in Figure 3-3, the front half of the source is the quadrant of one ellipsoidal source and the rear half of the heat source is the quadrant of

another ellipsoidal heat source. Because the temperature gradient in front of the heat source is steeper than that trailing edge of the molten pool, the power density of the region in front of the arc centre and the region behind the arc centre is defined separately.

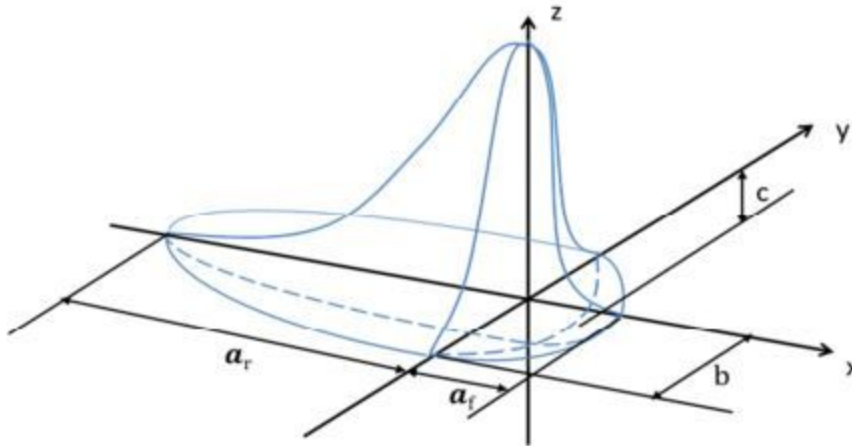


Figure 3-3 : Goldak's double ellipsoid heat source model

The power density distribution in the front quadrant can be described as:

$$q_f = \frac{6\sqrt{3}Qf_f}{\pi\sqrt{\pi}a_fbc} e^{\left[-3\left(\frac{x^2}{a_f^2} + \frac{y^2}{b^2} + \frac{z^2}{c^2}\right)\right]}$$

And the power density distribution for the rear quadrant is:

$$q_r = \frac{6\sqrt{3}Qf_r}{\pi\sqrt{\pi}a_rbc} e^{\left[-3\left(\frac{x^2}{a_r^2} + \frac{y^2}{b^2} + \frac{z^2}{c^2}\right)\right]}$$

Where, a_f and a_r are the front and rear length of the ellipsoid, respectively, b is the width and c is the depth of the heat source model respectively. Q is the energy input w.r.t the efficiency. The factor f_f and f_r are the distribution of power at the front and rear of the heat source respectively and is related as $f_f + f_r = 2$. The Goldak's heat source model is most utilized model for moving heat source and can be easily used with the change in weld parameters a, b and c , which can be calculated using the metallographic images.

3.1.2 Boundary Conditions

- The boundary conditions are a set of differential equations assigned at the boundary region of the model.
- The major heat losses due to conduction, convection and radiation are necessarily included in the model.
- Temperature-dependent mechanical and thermal properties are needed for performing simulation, especially yield stress and thermal conductivity. Phase change effects can be ignored. A cut-off temperature which equals to $0.5T_m$ to $0.7T_m$ is needed to be decided, where T_m is the melting temperature of the material.
- Goldak's heat source model is better for accurately simulating the physics of the welding process.
- Boundary conditions for the thermal analysis includes convection and radiation. If any cooling system is introduced, an equivalent convection coefficient can be used.
- Dense meshing should opt in weld vicinity zone. For large deformation to prevent, the shear locking reduced integration elements scheme can be considered.
- Element birth and death technique is better for simulating weld deposition process precisely.

3.1.4 Element Birth and Death Technique

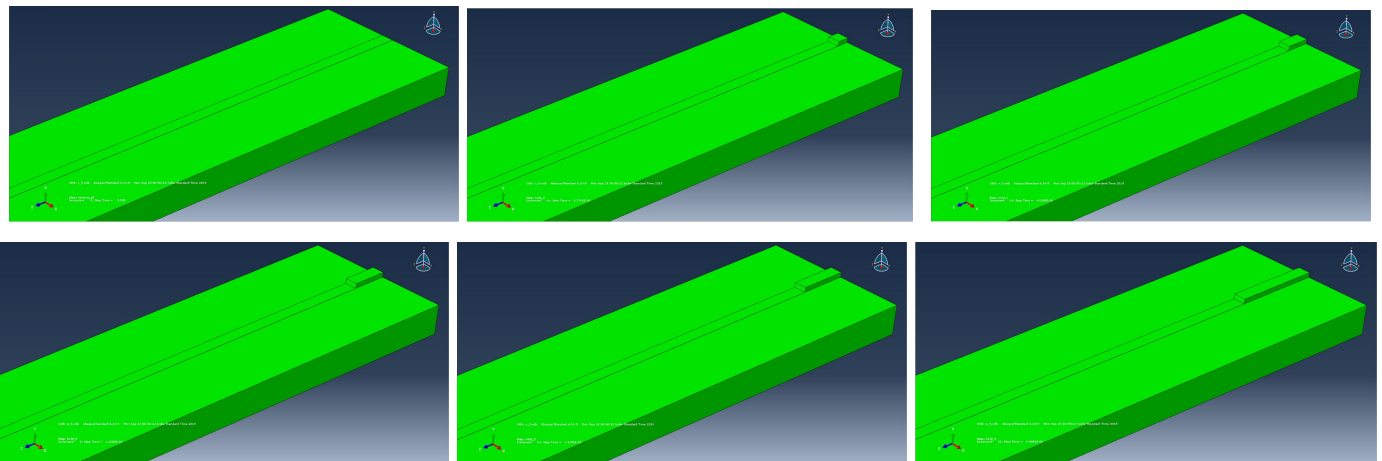


Figure 3-4: Depositions of the beads one by one using element birth technique

Elements can be added during the analysis using the Model change option. In order to add them later on, they need to be part of the initial geometry and first removed (deactivated). They can then be included (activated) later on. The steps used to remove or include elements (steps 1 and 4) are chosen to be very short, $1e^{-7}$ s. This way, the temperature field will not change noticeably during steps that are only meant to add or remove material. The model change option can be found in the Interaction module: create an interaction of type 'Model

change'. The figure 3-4 shown above shows that the filler material was simulated using the "element birth death technique", all the elements of the beads are deactivated in the first step of the analysis, and then the elements are activated sequentially following the heat source.

3.2 Transient Thermal Modelling

Heat transfer during the WAAM process includes heat generation by the welding arc, heat conduction in the deposited components, and the heat loss through the free surfaces and through the cooling system under the base plate. The welding arc was simulated as a volumetric heat source with a power density moving along with the torch. This moving heat source was generated with the user subroutine DFLUX in the ABAQUS code. The Goldak double ellipsoidal heat source (Goldak et al., 1984) as shown in Figure 3-3 was used to apply the heat to the additive manufacture deposits. The power density of the region in front of the arc centre and the region behind the arc centre was defined separately using the equation of the Power density distribution from the Goldak's heat source model. The parameter b was set using the value which equals to half of the width of the WAAM wall. The parameters c was set to the value which equals to the average layer height plus the penetration which was measured from the cross-section of the metallographic profile (as shown in Figure 3-5 (a)). And the values for a_f and a_r were estimated from weld pool surface ripple markings (as shown in Figure 3-5 (b)). Below are the goldak heat source parameters selected for the simufact welding simulations for the analysis of thermo-mechanical modelling.

- Front length $a_f = 2$ mm
- Rear length $a_r = 6$ mm
- Width $b = 2.5$ mm
- Depth $d = 3$ mm

Below are the welding parameters selected for experimental as well as simulation work these parameters were selected based after modelling and material selection .

- Velocity = 8.3 mm/sec
- $Q = 2245.83$ W
- Efficiency = 0.9

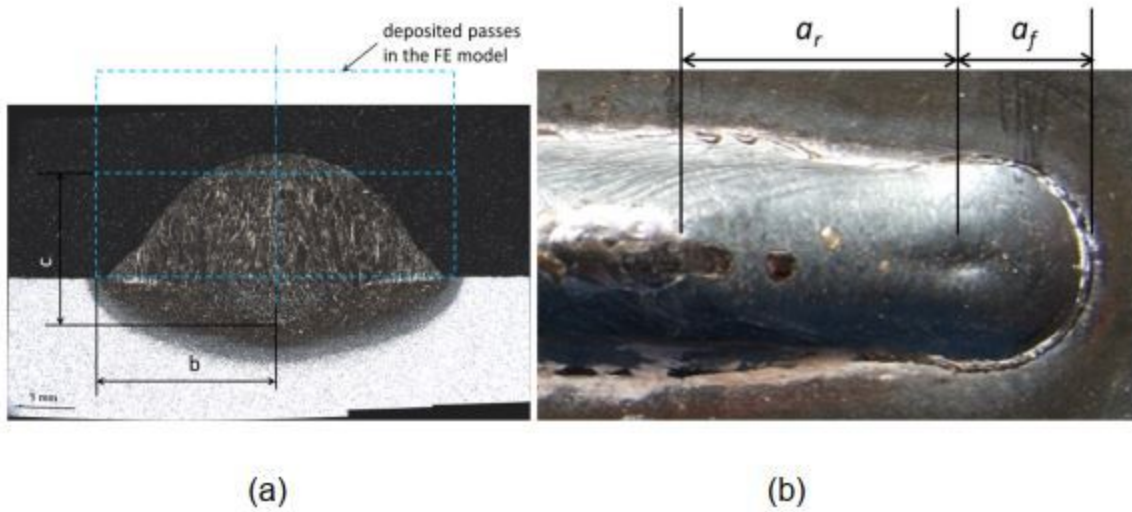


Figure 3-5 :The parameter settings for the Goldak double ellipsoidal heat source model. (a) Metallographic profile shows the settings for b and c ; (b) weld pool surface ripple markings for a_r and a_f

The main material used in the model is mild steel S355. The thermal properties were set for materials in the weld bead and base plate (as shown in Table 3-1). Temperature dependent thermal conductivity and specific heat were taken as the reference given in the Table. The specific heat was reduced when the temperature is above 723°C due to the phase transformation in this region. An artificially high thermal conductivity is used for temperatures greater than 1500°C to capture the convective heat transfer caused by the fluid flow in the weld pool. Constant material density at room temperature with a value of values to 7860 kg/m^3 was used in the simulation. The latent heat of fusion was accounted with the value of 270 kJ/kg between the solidus temperature 1450°C and the liquidus temperature 1500°C .

Temperature(°C)	Thermal conductivity (W/m°C)	Specific heat (J/Kg°C)
20	52	480
100	51	507
200	48	532
300	44	574
400	43	624
500	39	703
600	35.6	788
700	32	870
723	28	798
850	26	679
900	26.4	658
1250	30	666
1450	30	666
1500	120	670
2000	120	670

Table 3-1 : Detailed thermal properties of S355

Figure 3-6 shows the thermal boundary conditions that were setup in this study. The heat loss due to radiation and convection is modelled in ABAQUS using the keywords *RADIATION and *FILMS respectively. The radiation coefficient and the convection coefficient were assumed independent of the temperature and were set to 0.2 and 5.7 W/(m²K), respectively. The heat loss through the cooling system under the base plate was modelled with an equivalent convection coefficient. This coefficient was found by running a series of numerical trials, and tuning the value so that the predicted temperature profiles matched the experimental results. A value of 300 W/(m²K) gave the best match with the experiments. The parameters for heat loss were not applied to the longitudinal mid-plane because of the symmetry thermal boundary. In reality the clamps can also conduct some heat, however this was considered insignificant as the contact area of the clamps and the base plate was very small. Thus, the heat loss through the clamping devices was ignored in the model. The initial temperature was set at room temperature 20 °C. The Stefan-Boltzmann constant was set to 5.67x10⁻⁸ J/ (m²K).

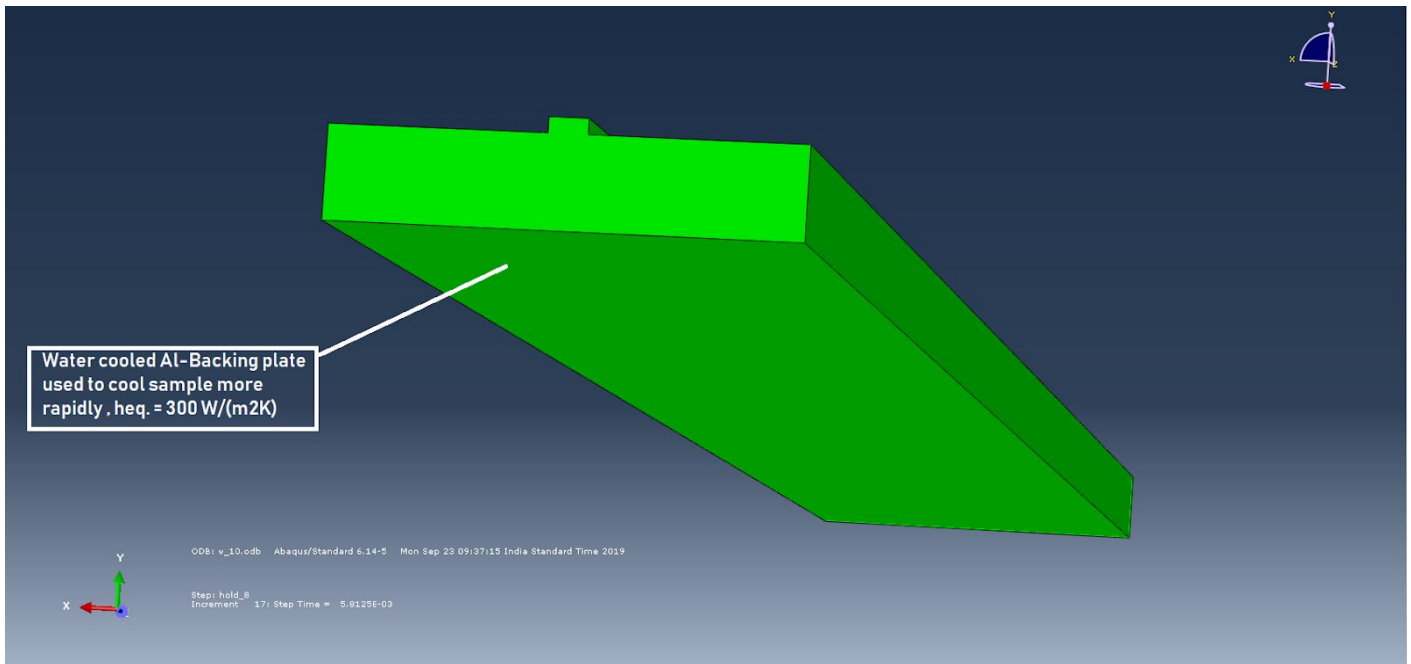
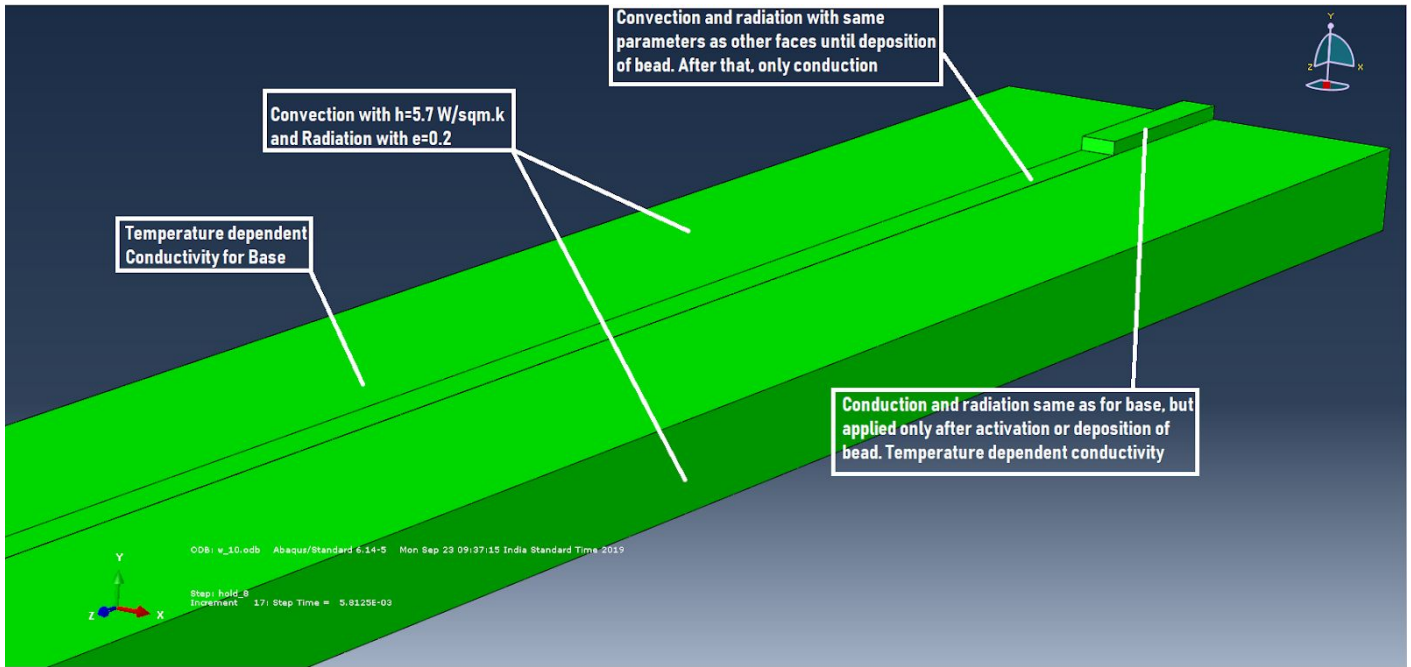


Figure 3-6 : Thermal Boundary conditions

3.3 Implementation of Transient Thermo-mechanical model

The thermo-mechanical analysis of the WAAM process in this chapter follows the procedure shown in Figure 3-7. The same FE meshes were employed in both thermal model and mechanical model with different element type. A 3D transient thermal analysis was

conducted first, and the thermal results were loaded in a plastic-elastic model for calculating residual stresses and distortions.

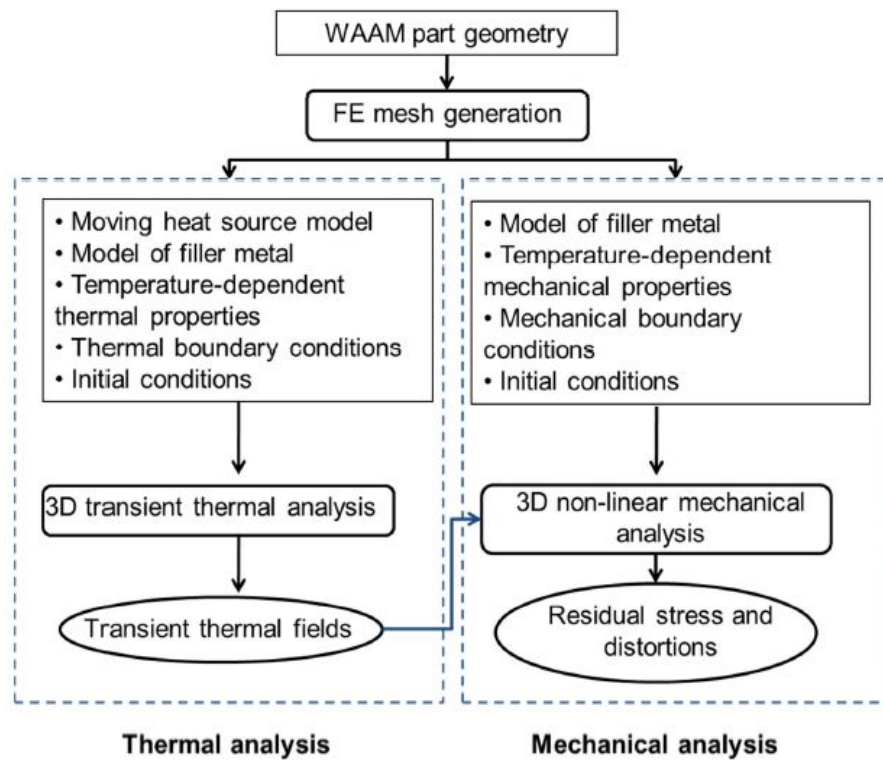


Figure 3-7: Procedure of transient thermo-mechanical modelling of the WAAM process.

3.4 Transient Mechanical Modelling

In the mechanical analysis of the model, yield stress plays a major role in the welding simulation. It has a significant effect on the residual stresses and distortions. Thus, accurate temperature dependent yield stresses is used for the model. Temperature-dependent Young’s modulus and thermal expansion coefficient values were also utilised in the mechanical model. The phase transformations are ignored in this study, as it has an insignificant effect on the welding residual stress for mild steel. To avoid difficulties in convergence, a ‘cut-off temperature’ of 1000°C was used in the material model. Young’s modulus and the yield stress of the material remain at the same value for temperatures above the cut off temperature. The detailed temperature-dependent mechanical properties of S355 are listed in Table 3-2 and Table 3-3.

Temp. (°C)	Poisson's ratio	Temp. (°C)	Thermal expan. coeff. (1/°C)
20	0.29	20	1.20E-05
200	0.295	1000	1.50E-05
400	0.3	1500	1.50E-05
600	0.32		
800	0.35		
1000	0.39		
1500	0.39		

Table 3-2 : Detailed temperature-dependent thermal expansion coefficient, and Poisson's ratio of S355

Temp. (°C)	Young's Modulus (GPa)	Yield Strength (MPa)			
		Filler metal	Filler metal ($\epsilon_p = 0.01$)	Base metal	Base metal ($\epsilon_p = 0.01$)
20	206	450	520	350	420
100	203	450	520	330	400
200	201	420	500	305	380
300	200	390	450	270	350
400	165	320	370	230	290
500	100	260	300	180	230
600	60	170	215	125	160
700	40	60	100	60	100
800	30	50	80	60	60
900	20	50	50	60	60
1000	10	50	50	60	60
1500	10	50	50	60	60

Table 3-3 : Detailed temperature-dependent Young's Modulus, and yield strength for the filler material and base plate

Continuous filler metal deposition changes the rigidity of the component as the solidification front advances with the weld pool. This gradually increased rigidity needs to be correctly developed in the model otherwise false weld distortion may be generated. Thus, the same “element birth technique” to the transient thermal model was also utilised in the mechanical model for simulating the deposition process of the filler material. The same number of computational steps and step durations of the thermal model were utilised in the mechanical simulation for the heating and cooling cycles. Another step was utilised at the end for simulating the mechanical performance after the clamps are released.

RESULTS AND CONCLUSIONS

While fabricating components using WAALM the first layer is deposited on base plate at room temperature while next layers are being deposited at a temperature much higher than room temperature i.e. the temperature of previously deposited beads with other perspective every layer is subjected to different heating loads which may result in residual stresses and change in properties so while depositing the estimation of interlayer cooling time is required to reach the steady state temperature which is needed to be calculated for the deposition of the next layer.

This analysis also considers the time temperature analysis of the certain points taken in the model in the multipass multilayer bead deposition to examine what is the temperature reached after each layer deposition. Figure 4-1 below shows the points (TP1, TP2 & TP3) directly at the base plate surface of the model to know its temperature histories-

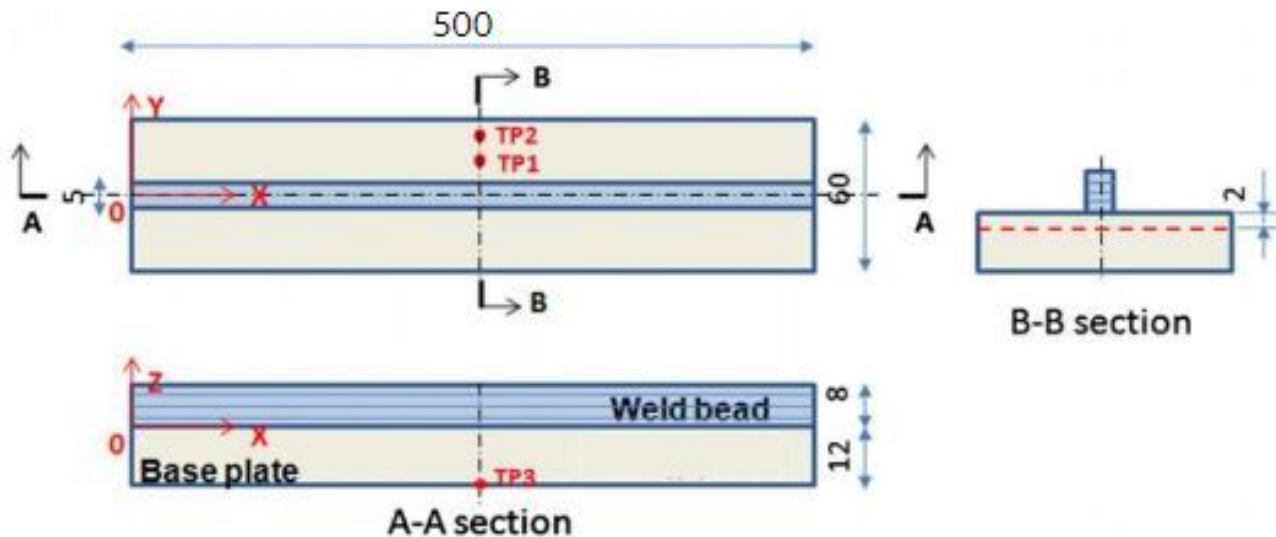


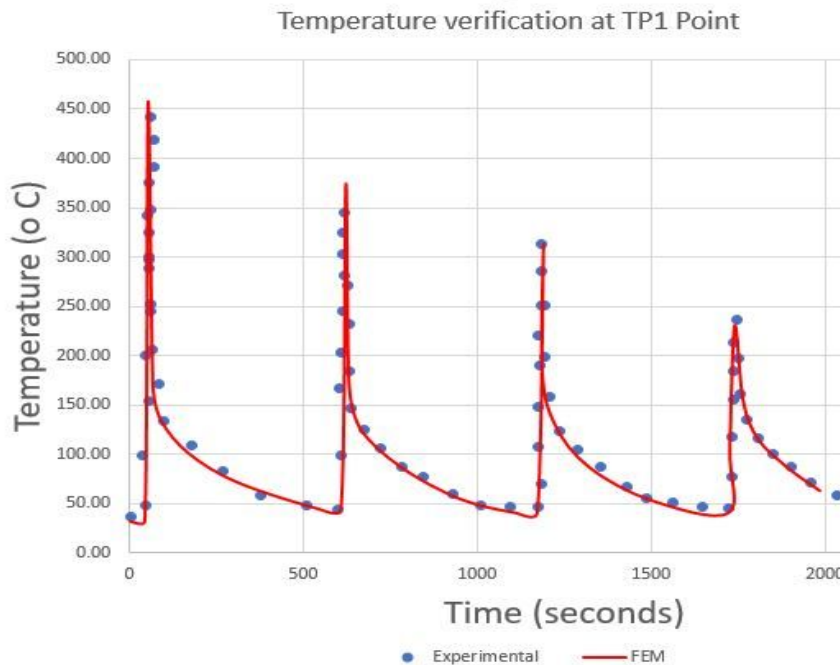
Figure 4-1: Nodes positions to know their Temperature histories

4.1 Temperature Histories of the certain points

The time temperature analysis was done to analyse the temperature profile with time. The total time for deposition was almost 2200 seconds (for 4 layers) and the first layer deposition took one fourth of the total time i.e. approximately 550 seconds. The Time-temperature plot was constructed using the points taken on the trajectory. Figure 4-2 shows the comparison between the numerical thermal histories and the experimental thermal histories at the four measuring positions on the base plate which are demonstrated in Figure 4-1. The predicted temperatures were extracted from the nodal points in the model where the thermocouples were placed in the experiment to verify the results.

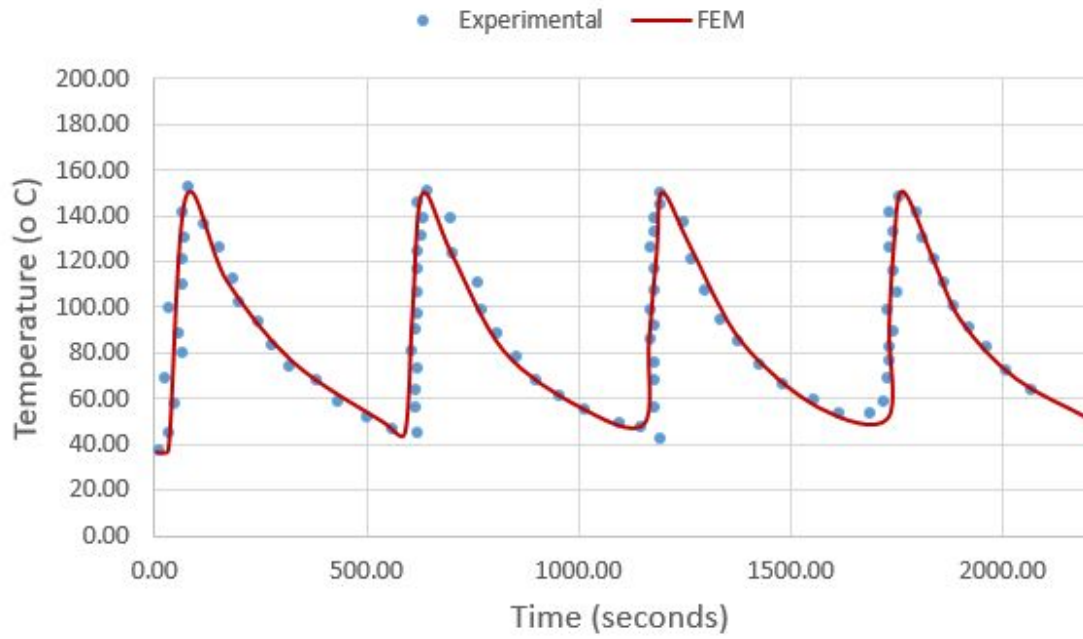
From the comparison, one can see that the transient thermal models give accurate predictions of the temperatures at the four thermocouple positions. Not only the peak temperatures are accurate, but the predicted heating and cooling rates are also well correlated to the measurements. From the graphs, we can conclude that the peak temperatures at the considering nodes 1 and 3 are decreasing due to reason of the distance between the nodes considered and the torch depositing the layers is increasing.

Figure 4-2: Temperature Histories using FEM & verification on the measuring positions (a) at TP1, (b) at TP2 & (c) at TP3



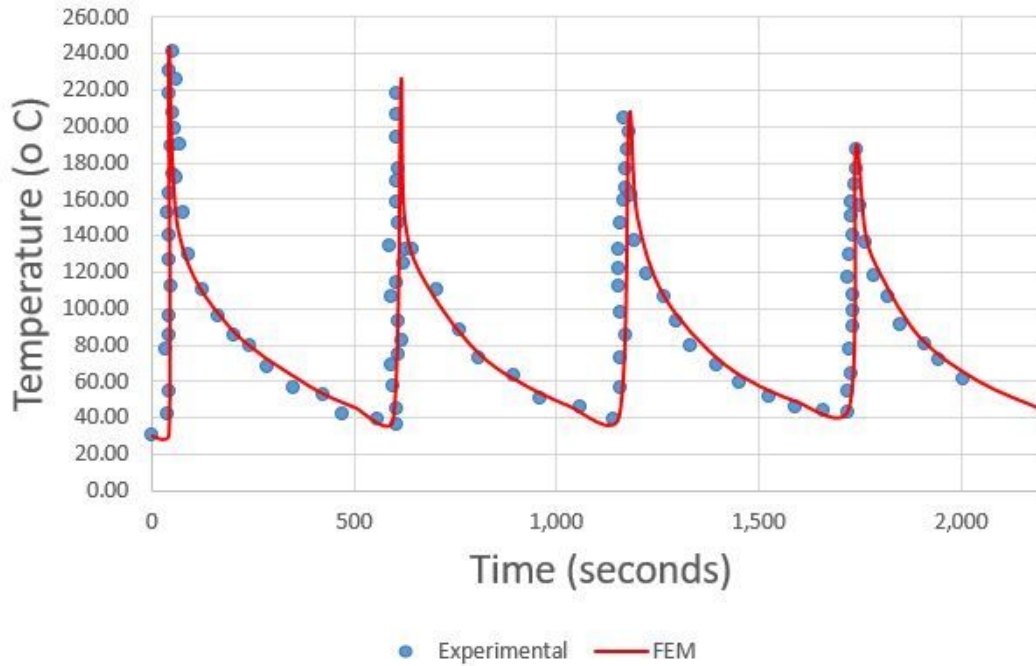
(a)

Temperature verification at TP2

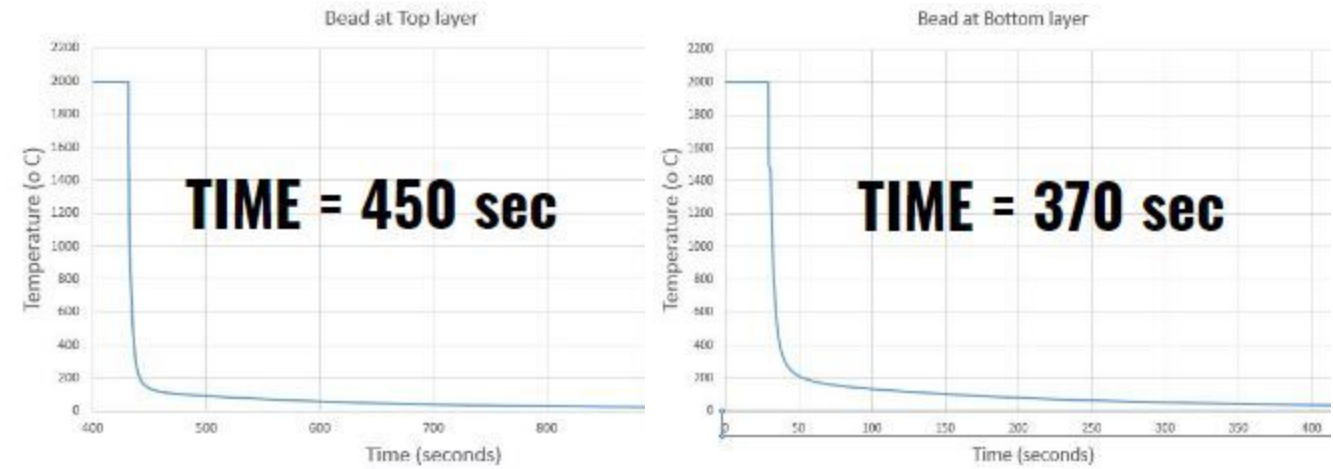


(b)

Temperature verification at TP3 Point



(c)



(d)

In the figure (d), the graphs showed the cooling time of the two nodes , one at the bottom of the layer and the other at the top of the layer. We observed that the cooling time taken by the two beads are different. The time taken by the top layer is more as compared to the bottom layer which should be the result as the bottom node is near the base plate through which most of the heat will dissipate, hence time taken for the cooling is less in bottom bead.

4.2 Mechanical Analysis Results:

Figure 4-3 (a) illustrates the predicted longitudinal residual stress of the four layer walls with clamping. From the mid-plane cross section shown in Figure 4-3(b) one can see that tensile stresses are distributed nearly uniformly across all the layers of the deposited wall. The stresses in the base plate adjacent to the deposited wall are also tensile, and the longitudinal stresses go into compression near the bottom of the base plate. The magnitude of the compressive stress is greatest where clamping has been applied due to the restraint in this region (shown in Figure 4-3(a)). There is a significant distortion of the component and relaxation of the stresses after the clamping was removed which is illustrated in Figure 4-3(c) and Figure 4-3(d). The stress at the top of the deposited wall has a much lower value than at the interface due to the bending distortion of the sample. This distortion also causes the compressive stress at the bottom of the base plate to go into tension.

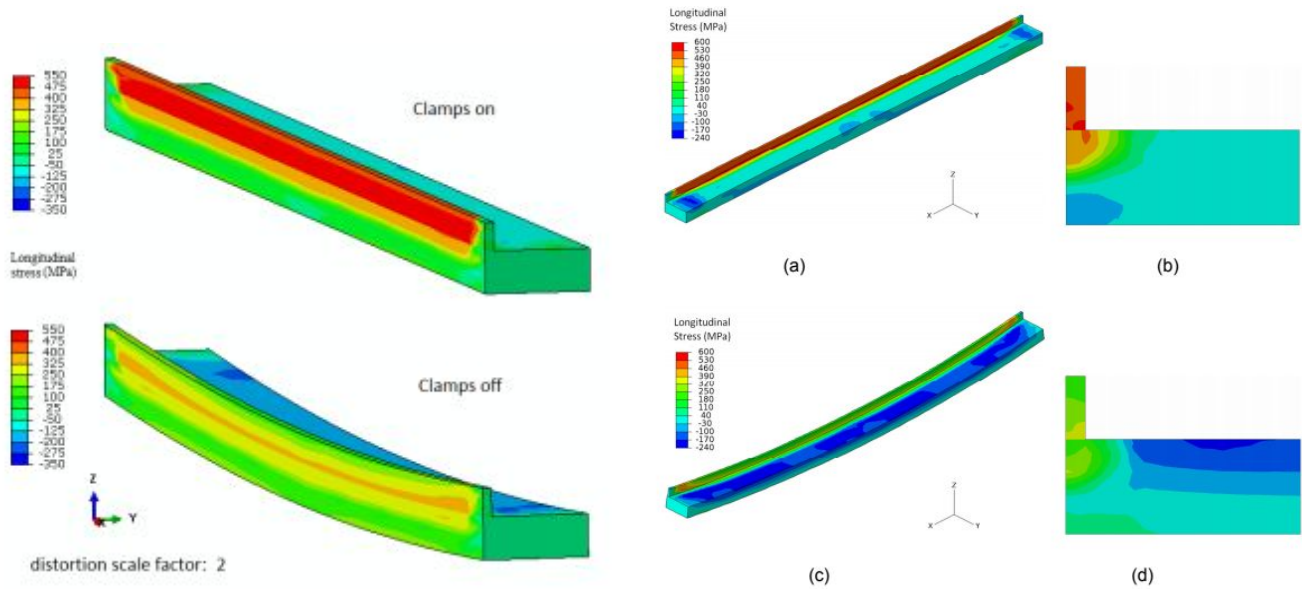


Figure 4-3: Longitudinal stress predictions of the 4 layer WAAM wall component: (a) with clamps; (b) cross section of (a); (c) after clamps are removed (deformation factor: 5); (d) cross section of (c).

To have an overall check of the mechanical results, the predicted distortion along the long edge of a four layer wall was compared with the measured distortion from the two long edges of the sample. Figure 4-4 shows that the predicted distorted shape agrees with the experimentally measured distortion. The distortion magnitude at the start of the component is slightly higher than it is at the stop end. This is because the rigidity of the component is continuously increasing during the deposition process. The rigidity of the component is higher when the whole layer of material added to the part which results in a lower distortion. This phenomenon can be correctly captured by the mechanical FE model using the “element birth” technique.

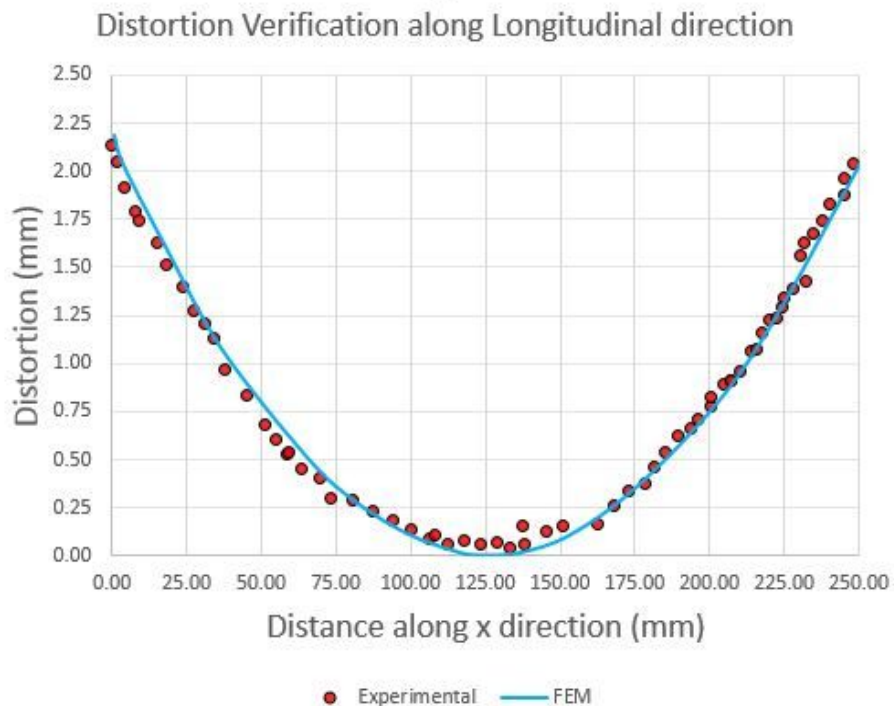
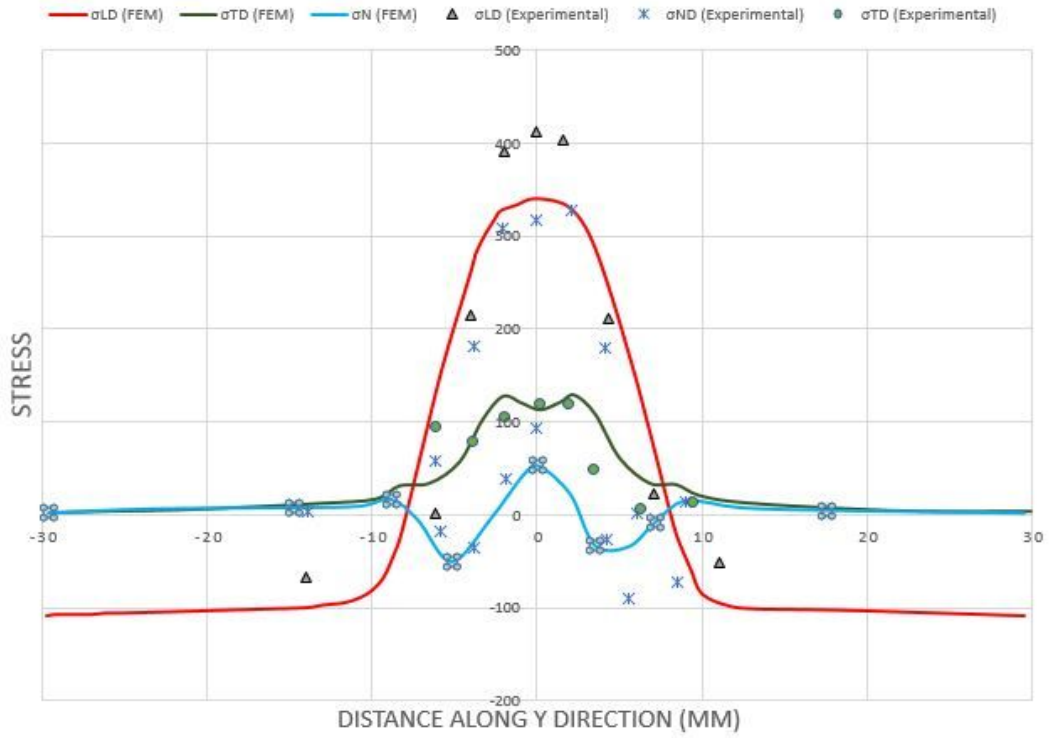


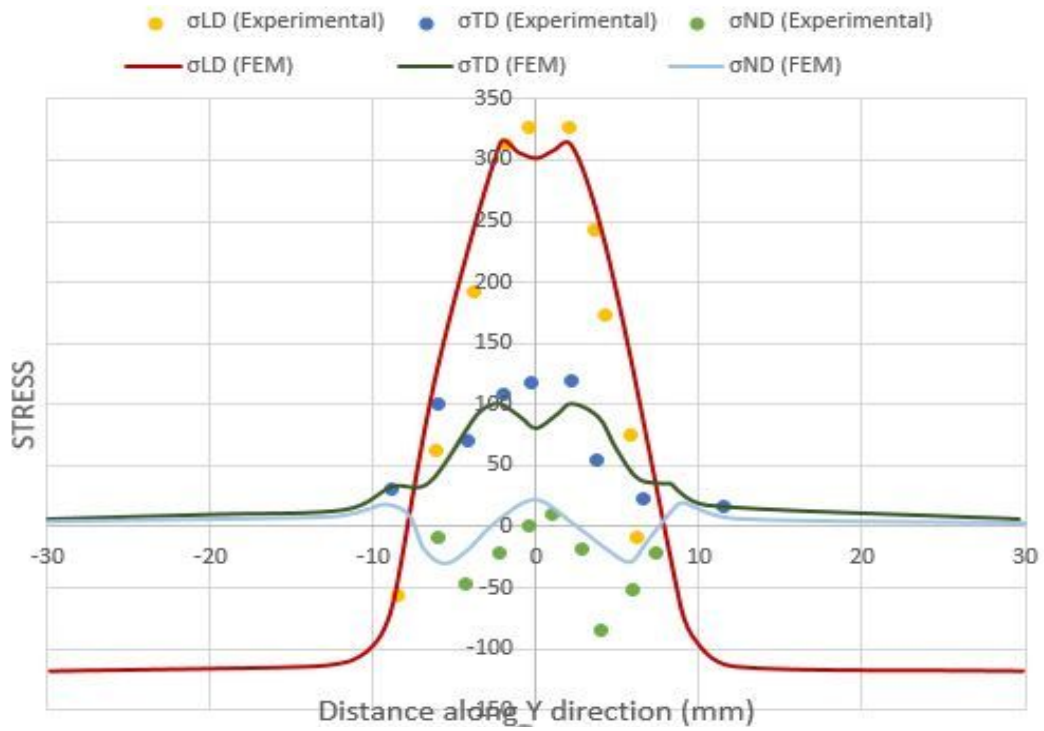
Figure 4-4: Verification of Distortion along Longitudinal Direction

Detailed validation of the residual stress data was provided by comparing the computational results for different numbers of deposited layers with those from experimental measurements. Figure 4-5 shows the comparison on the base plate. In both the modelling and experimental results the clamps have been removed, and three principal directions have been considered namely: longitudinal (σ_{LD}), transverse (σ_{TD}), and normal (σ_{ND}). It can be clearly seen that the longitudinal stress dominates over the transverse and normal stresses. The material around the heating line has large longitudinal tensile stresses. Along the transverse direction, the longitudinal stress becomes compressive in the area about 8 mm away from the heating line. However, the magnitude of the longitudinal tensile stress around the heating line is significantly higher than the surrounding longitudinal compressive stress. Transverse residual stresses are much smaller compared to the longitudinal stresses (shown in Figure 4-5). The transverse stress reaches its peak value close to the heating line and gradually reduces to zero towards the outer rim of the plate. The normal residual stresses are insignificant compared to the stresses of the other two directions. The FE predictions match the experimental results well in all cases except the 1 layer wall where the model underpredicts the stresses. Moreover, there is a more significant reduction in the experimentally measured stresses between the 1 and 2 layer walls, than in the stresses predicted by the models. A possible explanation is that the model does not fully capture the microstructural changes which occur in the actual material.

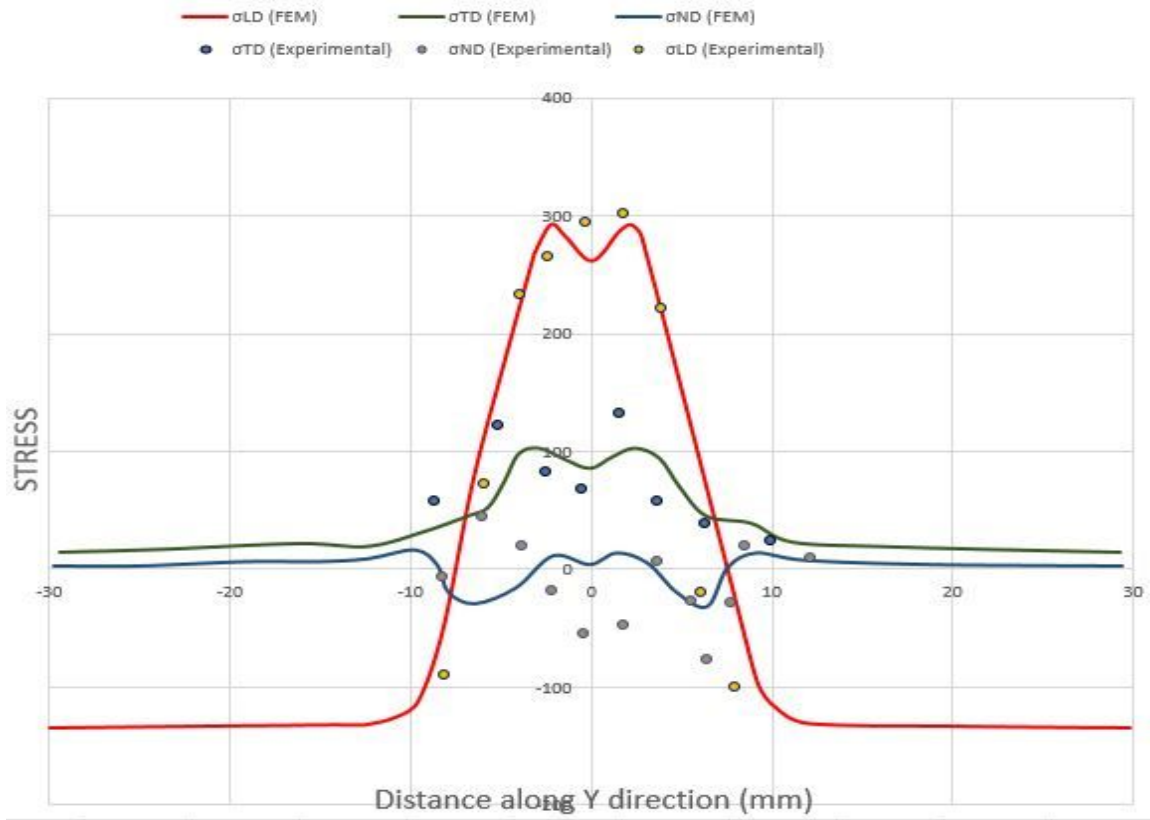
Figure 4-5: (a) Principal stress distribution along Transverse direction with 1 layer deposition, (b) Principal stress distribution along Transverse direction with 2 layers deposition, (c) Principal stress distribution along Transverse direction with 3 layers deposition.



(a)



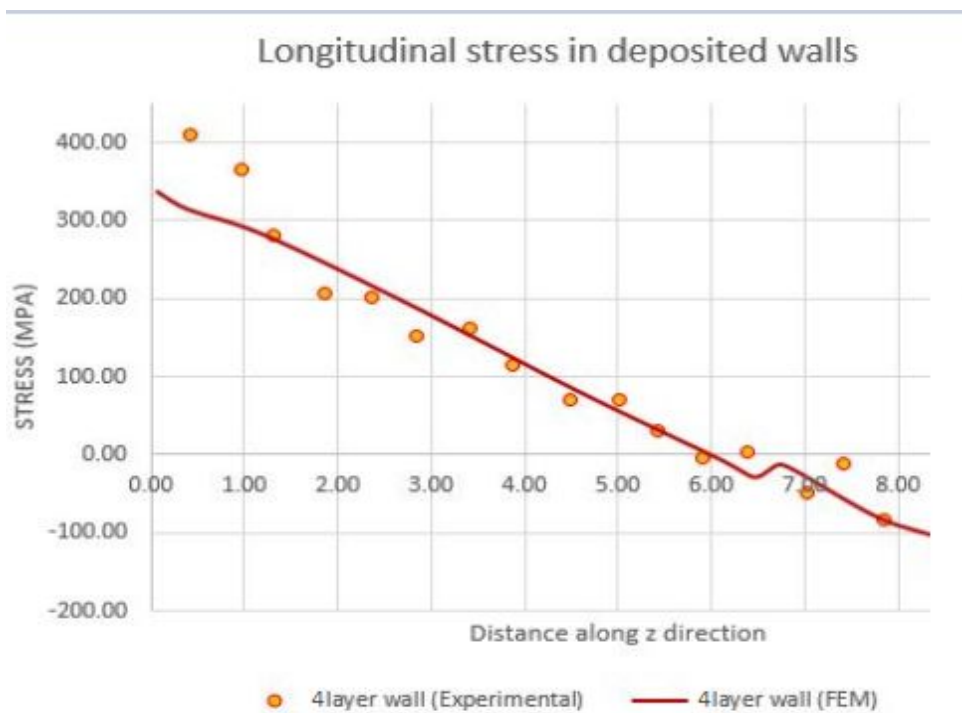
(b)



(c)

The comparison of the experimental measurement and the numerical prediction of residual stress distribution on the deposited wall on 4 layers beads is shown in Figure 4-6. The comparison was made on the longitudinal stress because it is dominant over the stresses from the other two directions. It shows that in general the predicted stress has the similar distribution as the measured result with a deviation near the base of the deposited wall. The possible reason of this error is that the complex dilution of the filler material and the base plate was ignored in the model. The maximum tensile stress was located in the base of the deposited wall. It decreased with the increased distance along the z direction and turned to compressive stress after a certain height.

Figure 4-6: Variation of Longitudinal Stresses along Z-direction (4 Layers of 2 mm each)



4.3 Summary

This project involves the thermal and mechanical analysis of the WAALM with the help of ABAQUS software by selecting the points on the base plate and the beads at the lower and upper layers deposited and studying the temperatures of those beads. It also investigates the effect of neighbourhood deposition on the adjacent beads and studies the time required to reach steady state temperature for base plate on subsequent deposition. In later part of the work a thermal model was developed to predict the interlayer cooling time between successive layers to make it reach at steady state temperature. Then, with the help of these temperature histories, we predicted the mechanical distortions and residual stresses that will be developed in the model after unclamping.

4.4 Conclusions

It can be concluded that whether or not the residual stresses can be developed in the material is decided by the magnitude of the peak temperatures that the material experienced during the

deposition. If the peak temperature of the material is high enough to generate plastic flow, then tensile stress will be developed after the material cools down to the room temperature. Otherwise the stress evolution in the materials will be only elastically which cannot generate residual stresses.

4.4 Scope for Future Work:

As most of the studies on the mechanical properties of the WAAM components are on small scale samples, a study of how these properties change when scaled up in size will be of relevance. A better understanding of the temperature profile during weld-deposition can be arrived at by employing enhanced instruments for better recording and control of temperature data of base plate and the subsequent layers. Some generic and universal guidelines can be evolved for a wider set of geometries so that simulations can be minimized. The fabrication of large products is a subject of concern to manufacture them using WAAM and further studies will be required to obtain better accuracy products.

References :

1. Thermo-mechanical analysis of Wire and Arc Additive Layer Manufacturing process on large multi-layer parts J. Ding*1, P. Colegrove2, J. Mehnen1, S. Ganguly2, P.M. Sequeira Almeida2, F. Wang2, and S. Williams2
2. ABAQUS Inc: available at: <http://www.abaqus.com>
3. J. Goldak, A. Chakravarti, M. Bibby, New Finite Element Model for Welding Heat Sources, Metall. Trans. B, 15B (1984), 299-305
4. Thermo-mechanical Analysis of Wire and Arc Additive, Manufacturing Process, Jialuo Ding, PhD thesis, Academic Year: 2008- 2012, CRANFIELD UNIVERSITY